Inhibition of Premixed Methane–Air Flames by Fluoromethanes

G. T. LINTERIS*
Fire Science Division, Building and Fire Research Laboratory, National Institute of Standards and Technology, Gaithersburg, MD 20899

L. TRUETT
1901 Tenth Street, WL/FIVS, Wright-Patterson AFB, Dayton, OH 45433

This paper presents the first calculations and measurements of the burning velocity of premixed hydrocarbon flames inhibited by the three one-carbon fluorinated species CH_2F_2, CF_3H, and CF_4. The chemistry of these agents is expected to be similar to that of some agents that may be used as replacements for CF_3Br, so that studying their behavior in methane flames provides an important first step towards understanding the suppression mechanism of hydrocarbon fires by fluorinated compounds. The burning velocity of premixed methane–air flames stabilized on a Mache–Hebra nozzle burner is determined using the total area method from a schlieren image of the flame. The inhibitors are tested over a range of concentration and fuel-air equivalence ratio, ϕ. The measured burning velocity reduction caused by addition of the inhibitor is compared with that predicted by numerical solution of the species and energy conservation equations employing a detailed chemical kinetic mechanism recently developed at the National Institute of Standards and Technology (NIST). Even in this first test of the kinetic mechanism on inhibited hydrocarbon flames, the numerically predicted burning velocity reductions for methane-air flames with values of ϕ of 0.9, 1.0, and 1.1 and inhibitor mole fractions in the unburned gases up to 0.08, are in excellent agreement for CH_2F_2 and CF_4 and within 35% for CF_3H. The numerical results indicate that the agents CF_3H and CH_2F_2 are totally consumed in the flame and the burning velocity is reduced primarily by a reduction in the H-atom concentration through reactions leading to HF formation. In contrast, only about 10% of the CF_4 is consumed in the main reaction zone and it reduces the burning velocity primarily by lowering the final temperature of the burned gases.

INTRODUCTION

Halogenated hydrocarbons containing bromine are effective [1] and widely used as fire suppressants. Because of their destruction of stratospheric ozone, however, the production of these agents, the most popular being halon 1301 (CF_3Br) will be discontinued in 1994. There exists a need to develop alternatives to these halons, to establish the relative effectiveness of alternative inhibitors, and to understand the mechanism of inhibition of the new agents. The agents that are currently being considered are mostly fluorinated and perfluorinated alkanes. This article describes measurements of the reduction in burning velocity of premixed methane–air flames with the addition of three fluoromethanes (CF_4, CF_3H, and CH_2F_2) that demonstrate some of the characteristics of the alternatives, while having structures simple enough so that their chemistry can be described by a recently developed kinetic mechanism. Methane, although its oxidation pathway is somewhat different from that of larger alkanes, was selected because its simple structure is amenable to modeling. Important insights into the chemical and physical mechanisms of inhibition by fluorinated agents in hydrocarbon flames can be obtained by studying these fuels and agents. As the model is further developed and tested, experiments and calculations will be performed for larger fuels and agents.

BACKGROUND

Early studies of the inhibitory effects of halogenated hydrocarbons on flames were conducted in premixed systems. The premixed laminar burning velocity is a fundamental parameter describing the overall reaction rate, heat release, and heat and mass transport in a flame. In addition, the reduction in the pre-

* Corresponding author.

COMBUSTION AND FLAME 105: 15–27 (1996)

Published by Elsevier Science Inc.

0010-2180/96/$15.00
SSDI 0010-2180(95)00152-V

mixed flame burning velocity is useful for understanding the mechanism of chemical inhibition of fires since diffusion flames often have a stabilization region that is premixed, and good correlation has been found between the reduction in burning velocity and the concentration of inhibitors found to extinguish diffusion flames [2]. Premixed flame burners have flow fields that are relatively easily characterized, making interpretation of the inhibitor's effect on the overall reaction rate straightforward. Numerous groups [3–6] determined the influence of halogenated methanes on the flammability limits of hydrocarbon–air mixtures. The magnitude of the inhibitory effect and its dependence on halogen type and stoichiometry generally indicated a chemical rather than thermal mechanism.

Simmons and Wolfhard [6] studied the flammability limits of methane–air mixtures with bromine and methyl bromide inhibitors and showed that methyl bromide influenced the limits of flammability in the same manner as equivalent amounts of bromine and methane, indicating that the decomposition products of the halogenated methanes are responsible for the action. Garner et al. [7], Rosser et al. [8], and Lask and Wagner [9] measured the reduction in burning velocity of various burner-stabilized hydrocarbon–air flames with addition of several halogenated methanes, halogen acids and halogen dimers. In later work, Niioka et al. [10] experimentally investigated the effect of CF_3Br on the extinction velocity of opposed premixed C_2H_4 flames. The inhibitory effect was found to be more effective in rich flames than in lean flames. Mitani [11] used experimental results on the decrease of flame propagation speeds of premixed H_2–O_2–N_2 and C_2H_4–O_2–N_2 flames with CF_3Br addition to derive overall activation energies for the inhibition reactions, which correlated well with measured energies for key inhibition steps. All studies were in consensus that the magnitude of the inhibition was related to the number and type of halogen atoms present in the reactants, the concentration of the inhibitor, and the equivalence ratio ϕ; and that the effect was generally too large to be accounted for by thermal dilution effects. This conclusion was based on supporting calculations or measurements showing that the final temperatures in the inhibited flames were not low enough to account for the burning velocity reductions observed.

Detailed information on the inhibition mechanism of brominated species has been provided by flame structure measurements. Mass spectrometric measurements of stable species concentrations in premixed flames of methane and air were conducted by several investigators: Levy et al. [12] used HBr to inhibit a Bunsen flame and found that HBr inhibited methane consumption but not CO oxidation; Wilson [13] and Wilson et al. [14] performed low-pressure inhibited premixed flame studies with methyl bormide, HCl, HBr, Cl_2, and concluded that both CH_3Br and HBr act to reduce radical concentrations in the preheat region of the flame by competing with the chain branching reaction $H + O_2 = OH + O$, and that CH_3Br lowers the peak OH concentration to near equilibrium values, while uninhibited flames have the characteristic superequilibrium OH concentrations. Biordi et al. [15, 16] used a molecular-beam mass spectrometer to obtain stable and radical species concentrations as a function of position in low-pressure premixed flat flames of methane and air with and without addition of CF_3Br, and Safieh et al. [17] performed similar experiments with a low-pressure CO–H_2–O_2–Ar flame. The data and analyses of these researchers provided detailed kinetic information on the mechanisms of Br and CF_3 inhibition under low-pressure premixed, burner-stabilized conditions. Day et al. [18] and Dixon-Lewis and Simpson [19] studied the burning velocities and the rich flammability limits of H_2–O_2–N_2 and H_2–O_2–N_2O flames. Their experiments and numerical modeling showed that the thermodynamic equilibrium relationship for the reaction $H + HBr = H_2 + Br$ together with recombination steps involving bromine atoms are primarily responsible for the inhibition effect of HBr compared with HCl and HF, rather than competition with the branching reaction $H + O_2 = OH + O$. Westbrook [20–22] developed a detailed chemical kinetic mechanism for HBr, CH_3Br, and CF_3Br inhibition and performed numerical calculations of flame structure, testing the mechanism

using experimental burning velocity reductions and, to some extent, using measured species concentration profiles.

In the research described above, the inhibition is dominated by the chlorinated and brominated species; however, most of the proposed replacements for CF_3Br contain only carbon, hydrogen, and fluorine. Recently, studies have examined systems containing only fluorinated inhibitors. Vandooren et al. [23] performed molecular-beam mass spectrometer measurements in a low-pressure premixed flame of CO, H_2, O_2, and Ar inhibited by CF_3H, determined the destruction route for CF_3H, and obtained rate expressions for key inhibition reactions. da Cruz et al. [24] measured the burning velocity of moist CO flames inhibited by CF_3Br, $CFCl_3$, CF_2Cl_2, CF_3Cl, CF_3H, and CF_4, and found that the effectiveness depended most strongly on number of Br and Cl atoms, and that the inhibitor effectiveness correlated with the rate of reaction of the inhibitor with H-atom. Sheinson et al. [25, 26] obtained experimental data on the concentration of halogenated hydrocarbons necessary to extinguish co-flow heptane diffusion flames, and used these data to develop empirical models of the contribution of the atoms and molecular groups in the inhibitor to the chemical and physical mechanisms of inhibition. Using molecular beam mass spectrometer measurements in a low-pressure H_2–O_2 flame, Richter et al. [27] determined the destruction pathway for CF_3H and found the reaction paths important for CO, CO_2 and CF_2O formation and CO destruction. These studies indicated that CF_3H reduces radical concentrations in the flames and inferred the important inhibition reactions to be $CF_3H + H = CF_3 + H_2$ and $CF_3 + OH = CF_2O + HF$.

None of these studies examined fluorinated inhibition in premixed hydrocarbon flames. The present research extends the investigations of burning velocity reduction to fluorinated inhibitors in hydrocarbon flames and applies a newly developed kinetic mechanism to model the experiments. Trifluoromethane was selected because it is the smallest molecule that is representative of the fluorinated alkanes and provides the simplest species with which to understand the chemistry that is believed to proceed through the CF_3 radical. In addition, it is being considered as an agent suitable for total flooding applications because of its low toxicity. Difluoromethane is also relatively simple to model and shows the effect of higher hydrogen to fluorine ratio in the fuel and the decomposition pathway which proceeds through the species CHF and CHF_2. Fluoromethane is an example of a perfluorinated agent. These compounds have been argued to be inert (due to the absence of the hydrogen atom which is more easily abstracted than a fluorine). Although burning velocity data are not as sensitive a test of a particular reaction mechanism as are flame structure measurements, the burning velocity data of the present research are useful for a first examination of the performance of the NIST fluorinated-species kinetic mechanism in hydrocarbon flames. The numerical results are then used to determine the modes of inhibition of the three fluoromethanes implied by this mechanism, which may suggest important areas for model refinement and additional experiments.

EXPERIMENT

Numerous techniques exist for measuring burning velocities of flames, and there are good reviews in the literature [28, 29]. All of the flame and burner geometries employed, however, cause deviations from the desired one-dimensional, planar, adiabatic flame. In the present research, a premixed conical Bunsen-type nozzle burner is used. This method was selected for the flame speed measurements because its simplicity allows rapid assessment of the behavior of a number of halon alternatives. The low rate of heat loss to the burner, the low strain rate, and the low curvature facilitate comparisons of the experimental burning velocity with the predictions of a one-dimensional numerical calculation of the flame structure. The burning velocity in Bunsen-type flames is known to vary at the tip and base of the flame and is influenced by curvature and stretch (as compared to the planar burning velocity); however, these effects are most important over small regions of the flame. Although measurement of a true one-dimen-

sional, planar, adiabatic burning velocity is difficult, the relative change in the burning velocity can be measured with more confidence. Consequently, the burning velocity reduction in the present work is normalized by the uninhibited burning velocity. For comparison with the results of other researchers, the absolute burning velocities of the uninhibited flames are also presented.

The flame speed measurements are performed using a Mache-Hebra nozzle burner [30]. The burner consists of a quartz tube 27 cm long with an area contraction ratio of 4.7 (over a 3 cm length) and a final nozzle diameter of 1.02 ± 0.005 cm. The nozzle contour is designed to produce straight-sided schlieren and visible images which are very closely parallel. The burner is placed in a square acrylic chimney 10 cm wide and 86 cm tall with provision for co-flowing air or nitrogen gas (for the present data, the co-flow velocity is zero). Gas flows are measured with digitally controlled mass flow controllers (Sierra Model 860)[1] with a claimed repeatability of 0.2% and accuracy of 1%, which have been calibrated with bubble and dry (American Meter Co. DTM-200A) flow meters so that their accuracy is ±1%. The fuel gas is methane (Matheson UHP) and the inhibitors are trifluoromethane (Dupont), fluoromethane (PCR), and difluoromethane (Allied Signal). House compressed air (filtered and dried) is used after it has been additionally cleaned by passing it through an 0.01-μm filter, a carbon filter, and a desiccant bed to remove small aerosols, organic vapors, and water vapor. The product gas temperature of the uninhibited flames is measured with Pt/Pt 6% Rh–Pt/Pt 30% Rh thermocouples which are coated with Yttrium oxide to reduce catalytic reaction on the thermocouple surface. Measurements with two bead diameters (344 and 139 μm) allow correction for radiation losses.

For the present data, the visible flame height is maintained at constant value of 1.3 cm to provide similar rates of heat loss to the burner, while the desired equivalence ratio and inhibitor concentration are preserved. An optical system provides simultaneously the visible and schlieren images of the flame. A 512 by 512 pixel CCD array captures the image which is then digitized by a frame-grabber board in an Intel 486-based computer. The flame area is determined (assuming axial symmetry) from the digitized schlieren image using custom-written image processing software. The average mass burning velocity for the flame is determined using the total area method [29].

The experimental technique is similar to that used extensively by Van Wonterghem and Van Tiggelen [31]. The present burner, however, is larger, providing less curvature and strain; the flame holder is not water-cooled and the material (quartz) has a much lower thermal conductivity, reducing heat losses to the burner; the ratio of the flame height to the burner diameter is smaller so that there is less curvature, strain, and buoyancy-driven flow; and the burner is enclosed in a chimney with provision for any co-flow gas. The mass flow controllers provide additional flexibility in the operation of the burner.

MODEL

The structure of the inhibited premixed methane-air flame is calculated using currently available techniques [32–34]. The equations of mass, species, and energy conservation are solved numerically for the initial gas compositions of the experiments. The solution assumes isobaric, adiabatic, steady, planar, one-dimensional, laminar flow and neglects radiation and the Dufour effect (concentration gradient-induced heat transfer) but includes thermal diffusion. Molecular diffusion is modeled using mixture-averaged diffusion coefficients. The adopted boundary conditions, corresponding to a solution for a for a freely propagating flame, are a fixed inlet temperature of 298 K with specified mass flux fractions at the inlet and vanishing gradients downstream from the flame. The calculations employed a chemical kinetic mechanism recently developed at NIST

[1] Certain commercial equipment, instruments, or materials are identified in this paper in order to adequately specify the experimental procedure. Such identification does not imply recommendation or endorsement by the National Institute of Standards and Technology, nor does it imply that the materials or equipment are necessarily the best available for the intended use.

[35–36] for fluorine inhibition of hydrocarbon flames, which is based on earlier work [37–39]. The 83-species mechanism uses a hydrocarbon sub-mechanism and adds C_1 (200 reactions) and C_2 (400 reactions) fluorochemistry. The hydrocarbon submechanism has been updated to use GRI-Mech (31 species, 177 reactions; [40]), which more closely predicts our experimental uninhibited burning velocities. The fluorinated-species thermochemistry in references [35, 36] is from the literature when available and is otherwise estimated using empirical methods (such as group additivity) and through application of ab initio molecular orbital calculations. Fluorinated species reaction rates from the literature were used when available and these were extended to wider temperature and pressure ranges using RRKM and QRRK methods. Where no rate data were available, rate constants were estimated by analogy with hydrocarbon reactions. Although all of the reactions are not necessary to describe the present flames adequately, the comprehensive full mechanism is used for these initial calculations. Reduction of the mechanism will be performed later after more experimental validation. It should be emphasized that the mechanism adopted [35–39] for the present calculations should be considered only as a starting point. Numerous changes to both the rates and the reactions incorporated may be made once a variety of experimental and theoretical data are available for testing the mechanism.

RESULTS

The current data and calculations are extensions of results previously presented [41, 42]. Here, the experiments are conducted over a wider range of equivalence ratio and at greater inhibitor mole fractions and also include results for the inhibitor CF_4. In addition, the kinetic mechanism has been updated to correspond to that which will appear in references [35–36]. The radiation-corrected temperature of the uninhibited flames was measured at 4 mm above the flame tip to be 2054, 2075, and 2050 K for $\phi = 0.95$, 1.0, and 1.05 respectively, while the adiabatic flame temperature is calculated to be 2191, 2229, and 2234 K (note that the inhibited flame speeds themselves were measured for a slightly wider range of equivalence ratio, 0.9 to 1.1). In these measurements, the final temperatures are about 150 K lower than the calculated adiabatic flame temperatures (the adiabatic flame temperature is the same final temperature achieved in the calculation at a position far downstream). Heat losses to the burner, although important near the rim, are not expected to be large compared to the heat release integrated over the entire flame. The observed heat loss may be due to non-one-dimensional effects, radiation, or chemical non-equilibrium in the post-combustion gases. Nonetheless, since the temperature difference is not too great, it seemed most appropriate to model the flame as freely propagating rather than burner-stabilized (where heat losses, for example in a flat flame burner, are typically much greater).

The digitized images of the flames showed that both the schlieren and visible images are straight and parallel over all of the flame image for CF_3H and CF_4 at all inhibitor concentrations (the tip of the flame is not imaged in the current arrangement). Since the distance between the two images is related to the flame thickness, which is in turn related to the burning velocity, the burning velocity appears to be relatively constant over most of the flame. For CH_2F_2 at mole fractions above 6%, there is noticeable curvature in the schlieren image, indicating that non-one-dimensional effects may be more important.

Figure 1 presents the measured mass burning velocity (expressed as the equivalent flame velocity for flame propagation into reactants at 298 K) as a function of equivalent ratio for the uninhibited methane-air flame, together with the results of Rosser et al. [8] and Vagelopoulos et al. [43]. The present data are about 7% higher than the results of Rosser et al. for $\phi < 1.0$ and up to 30% higher for $\phi > 1.0$. Rosser et al.'s experiments were also performed in premixed Bunsen-type flames where stretch and curvature can influence the burning velocity. In the recent experiments of Vagelopoulos et al. [43], the measured burning velocities of the planar flames are extrapolated to zero stretch. For values of ϕ from 0.8 to 1.2 the present data are 3%–7% higher than their results. This discrepancy may result from cur-

vature and stretch in the present flame. Figure 1 also shows the burning velocity as a function of stoichiometry calculated using the present mechanism. Since the present analysis requires a large number of flame solutions using a very large mechanism, it was necessary to limit the number of active grid points in the solution to 70–80 (values of GRAD and CURV of 0.35 and 0.55 in the PREMIX code). As shown in Fig. 1, this produces a peak burning velocity in the uninhibited flame of 40.8 cm/s, which is 6% higher than the peak burning velocity of 38.7 cm/s which we estimate as the value obtained with an infinite number of grid points (a value of 38.9 cm/s is reported in Ref. 43). This slight loss in accuracy is acceptable considering the large time reduction for the calculations, and recalling that the burning velocity reductions are reported and compared as normalized burning velocity reductions. The agreement between the experiment and model is very good for the number of grid points used; however, using three hundred or more grid points gives burning velocities slightly lower, so that the experimental results would

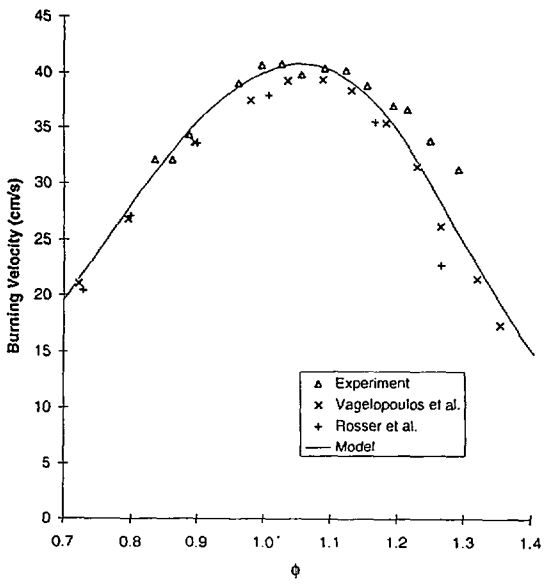

Fig. 1. Burning velocity determined using the total area method from the schlieren image of the premixed methane–air flame in the nozzle burner as a function of fuel–air equivalence ratio, together with the experimental results of Vagelopoulos et al. [43] and Rosser et al. [8]. The solid line is the numerically calculated burning velocity.

be about 7% too high for values of ϕ from 0.8 to 1.2. Nonetheless, this agreement is considered to be good, and is expected since GRI-Mech is being developed using existing experimental methane-air burning velocities and the present experimental results are close to those of other researchers.

The results for the flames inhibited by N_2, CF_4, CH_2F_2, and CF_3H are presented in Figs. 2a–2d respectively. The figures show the burning velocity of the inhibited flame (normalized by the burning velocity of the uninhibited flame) for values of ϕ of 0.9, 1.0, and 1.1 (here the equivalence ratio is calculated based on the oxygen demand of the fuel only). The mole fraction of the inhibitor in Figs. 2–2d, as well as in all other figures, refers to the entire reactant mixture: fuel + oxidizer + inhibitor. As a baseline case, Fig. 2a shows the results for a flame inhibited by N_2. The excellent agreement in Fig. 2a is again a consequence of the performance of GRIMECH. Most of the scatter in the plots of the experimental burning velocity results from flame fluctuations: the camera framing rate is 30 Hz and flame area is obtained from a single image; signal averaging would reduce this scatter.

In Figs. 2b–2d, the numerical results are presented in two ways: the solid lines present solutions which allow full chemistry, while the dotted lines present solutions in which the inhibitor is constrained to be inert so that only the thermal and transport properties of the flame are modified by the inhibitor. Experimental and numerical results are presented for inhibitor mole fractions up to 0.08 when possible; for the lean stoichiometry and the inhibitors CF_4 and CF_3H, flames could not be stabilized for inhibitor mole fractions above about 4%.

Figure 2b shows the results for CF_4. The lines are nearly coincident for the inert calculations at $\phi = 1.0$ and 1.1, and the reacting calculation at $\phi = 0.9$ and 1.0. The experiments show slightly more inhibition for richer flames, whereas the model shows more inhibition for the leaner flame. The calculation which assumes CF_4 to be inert shows slightly less inhibition than the solution that allows decomposition, but again, the difference is small. The

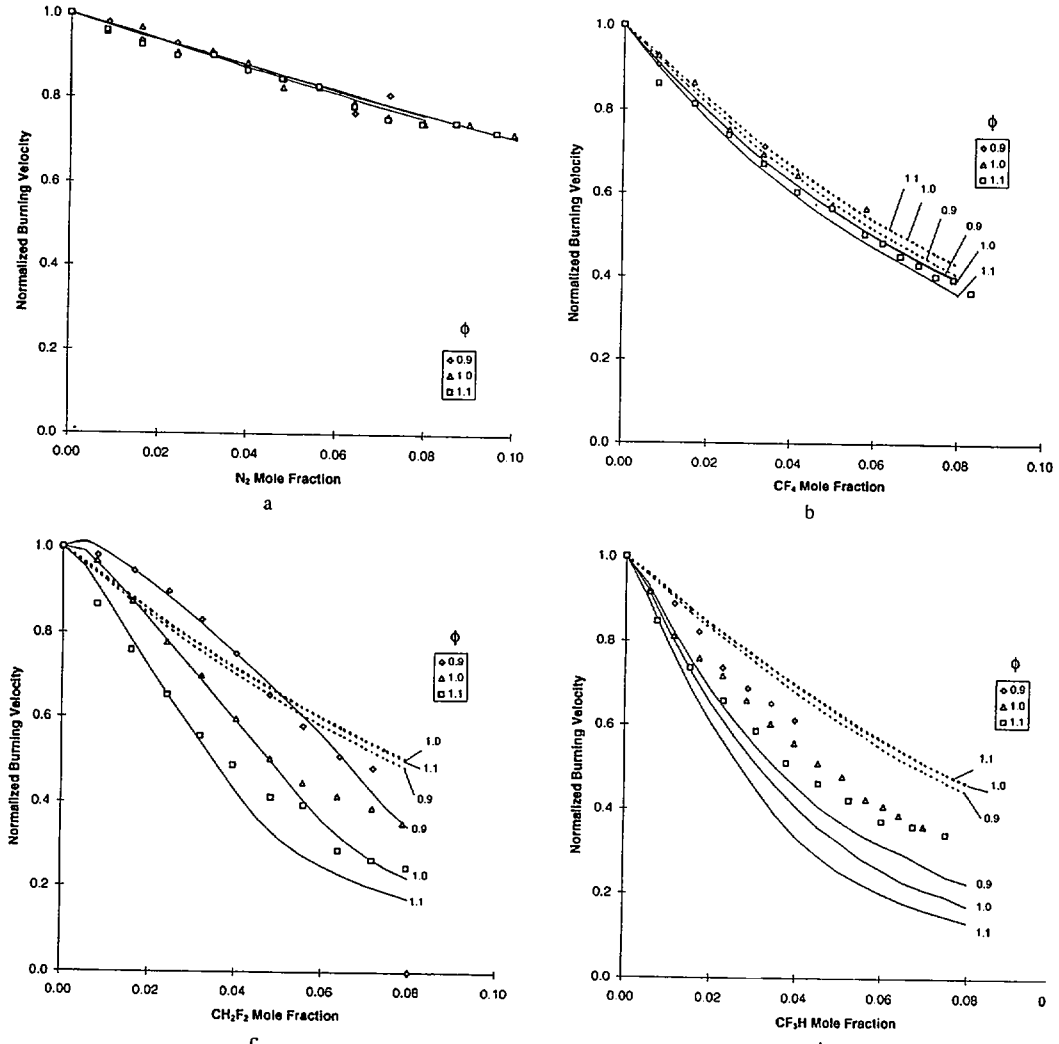

Fig. 2. Burning velocity of premixed methane–air flame normalized by the uninhibited burning velocity at the same stoichiometery as a function of the inhibitor mole fraction of the total reactant stream. Data are presented for the inhibitors N_2, CF_4, CH_2F_2, and CF_3H at fuel-air equivalence ratios of 0.9, 1.0, and 1.1. The symbols present the experimental data, the solid lines the results of the numerical calculation allowing inhibitor reaction, and the dotted lines the numerical calculation with the inhibitor present but non-reacting.

calculated burning velocity is in excellent agreement with the numerical solution which allows reaction of CF_4.

Figure 2c presents the results of CH_2F_2. Again, rich flames show more inhibition than the lean flames but the effect is large for CH_2F_2. The fuel effect of adding CH_2F_2 to lean flames increases the adiabatic flame temperature above the uninhibited case for low CH_2F_2 mole fractions, promoting a higher burning velocity. In competition with this effect is the slower kinetics caused by presence of the fluorine compounds as discussed below. Note that although the adiabatic flame temperature is higher for lean flames with up to 5% CH_2F_2, the burning velocity is still reduced relative to the uninhibited flame. The calculated burning velocities are very close to the measured values for CH_2F_2 mole fractions up to 5%; as the inhibitor mole fractions reach 8%, the calculations over-predict the burning velocity reductions by up to 17%.

The results for CF_3H are shown in Fig. 2d. The mechanism is showing the proper qualitative features of the inhibition including the dependence on stoichiometry and the reduced inhibitory effect at higher inhibitor mole fractions; however, the calculation is showing up to 20% more reduction in burning velocity than is observed in the experiments.

Figure 3 summarizes the calculated burning velocity for inhibition by CH_4 and CF_4, CH_2F_2, and CF_3H at $\phi = 0.9$ and 1.1; experimental results for CF_3Br [8] are included for comparison. All calculations predict that the rate of reduction in the burning velocity with addition of inhibitor becomes less at higher inhibitor concentrations, and predict a strong effect of ϕ on the inhibition effect. The fluoromethanes are much less effective than CF_3Br at reducing the burning velocity of methane–air flames at these equivalence ratios. Interestingly, all of the fluoromethanes are less efficient at reducing the burning velocity of the rich methane-air flames than methane itself. For the slightly fuel lean flames, the fuel effect (increasing burning velocity of lean flames with addition of the inhibitor) is larger for methane than for the fluoromethanes, yet upon entering the fuel rich regime, the effect of methane as an inhibitor again is greater than the fluoromethanes.

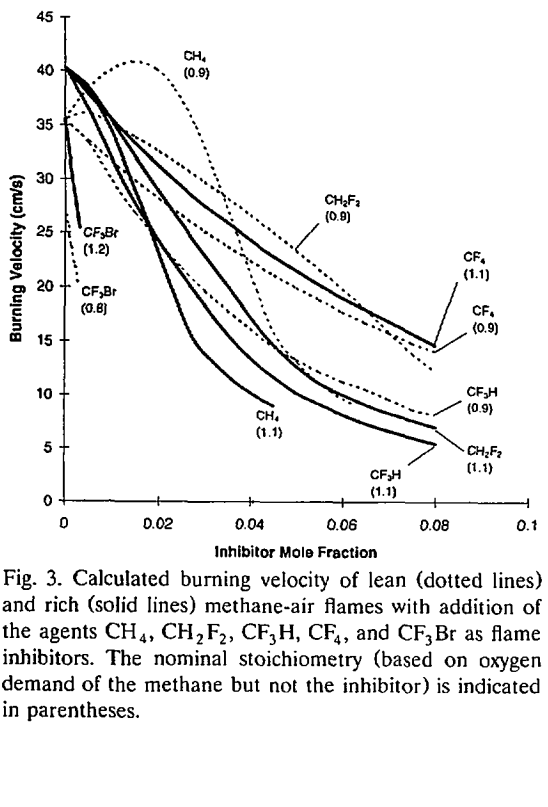

Fig. 3. Calculated burning velocity of lean (dotted lines) and rich (solid lines) methane-air flames with addition of the agents CH_4, CH_2F_2, CF_3H, CF_4, and CF_3Br as flame inhibitors. The nominal stoichiometry (based on oxygen demand of the methane but not the inhibitor) is indicated in parentheses.

DISCUSSION

In the present research, the burning velocity is the only parameter used to assess the kinetic mechanisms' performance. Since many of the reaction rates in the present mechanism are estimations, it is of interest to examine the sensitivity of the burning velocity to the fluorine reactions. Table 1 lists the fluorinated-species reactions for which the burning velocity sensitivity (normalized by the highest sensitivity) is greater than 2%, for CF_3H, CH_2F_2, and CF_4.

Figures 4a and 4b show the dominant reaction pathways for CH_2F_2, and CF_3H for $\phi = 1.0$ and an inhibitor mole fraction of 4% as deduced from the numerical calculations (integrating the reaction fluxes only over the primary reaction zone of the flame). The arrows

TABLE 1

First-Order Sensitivity Coefficient of the Burning Velocity with Respect to Fluorine Reactions Normalized by the Maximum Sensitivity of All Reactions (V_0 is the burning velocity, ω_I is the rate of reaction I), for 4% CH_2F_2, CF_3H, and CF_4 in Stoichiometric Methane–Air Flames

Agent	Reaction	$\frac{dv_0/d\omega_I}{dv_0/d\omega_I\|_{max}}$
CF_3H	$CO + F + M = CFO + M$	0.206
	$CHF_3 + M = CF_2 + HF$	0.203
	$CFO + H = CO + HF$	0.160
	$CF + O_2 = CFO + O$	0.088
	$CHF_3 + H = CF_3 + H_2$	0.052
	$CH_3 + CF_3 = CH_2CF_2 + HF$	0.047
	$CF + OH = CO + HF$	0.045
	$CFO + OH = CO_2 + HF$	0.034
	$CF + H = C + HF$	0.030
	$CH + HF = CF + H_2$	0.027
CH_2F_2	$CH_2F_2 + OH = CHF_2 + H_2O$	0.207
	$CHF + HF = CH_2F_2$	0.174
	$CHF_2 + HO_2 = CF_2O + OH + H$	0.104
	$CH_3 + CHF_2 = CH_2CHF + HF$	0.089
	$CO + F + M = CFO + M$	0.077
	$CFO + H = CO + HF$	0.069
	$CH + HF = CF + H_2$	0.056
	$CF + O_2 = CFO + O$	0.031
CF_4	$CF_4 + H = CF_3 + HF$	0.058

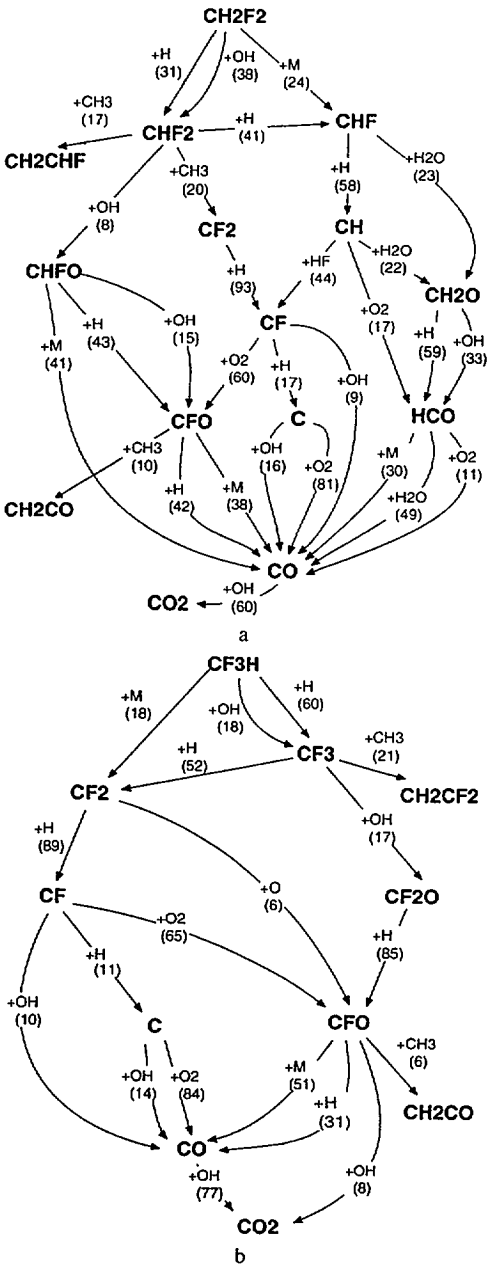

Fig. 4. Dominant reaction pathways for decomposition of the inhibitors CH_2F_2 and CF_3H in a stoichiometric premixed methane-air flame to which 4% inhibitor has been added. Each arrow connects a reactant and product of interest; for each reaction route, the reaction partner and the percentage of the reactant that goes through that route are indicated.

connect species of interest; next to the arrows are the second reacting species and the percent of the first reactant which goes through that route. Two-thirds of the difluoromethane reacts with H and OH to form CHF_2, while the remainder undergoes thermal decomposition to form CHF. Much of the CHF_2 reacts with H to also form CHF, which also reacts with H to form CH. About a sixth of the CHF_2 reacts with CH_3 to form CH_2CHF (whose consumption is not shown for clarity), while a fifth reacts with CH_3 to form CF_2 and CH_4. Rapid consumption of CHF_2 and CHF limit their peak concentration to about 137 and 52 ppm, respectively. About 40% of the CH reacts with H_2O and O_2 as in uninhibited hydrocarbon flames and is ultimately oxidized to CO. Interestingly, another 44% of the CH predicted to react with HF (often presumed to be inert in these flames) to form CF which then reacts with O_2 to form CFO, and with H to form C. The species CFO ultimately forms CO through reactions with H and OH and thermal decomposition.

The reaction pathway for CF_3H is noticeably different. Loss of hydrogen through reaction with H and OH leads to the CF_3 radical, most of which reacts with H atom to form CF_2 (in contrast, the work of Vandooren et al. [23] and Richter et al. [27] in carbon monoxide and hydrogen flames with 3% CF_3H predict the main reaction of CF_3 to be $CF_3 + OH = CF_2O + HF$). The methyl radical again reacts with about 20% of the fluorinated radical present in highest concentration, in this case CF_3 (218 ppm), to form a two-carbon fluorinated molecule (CH_2CF_2). Most of the CF_2 reacts with H-atom to form CF, which decomposes as in the CH_2F_2 case described above.

The reaction pathway for CF_4 is very similar to that of CF_3H. However, the decomposition of CF_4 is slow, and only about 10%–29% of the CF_4 is consumed by the end of the primary reaction zone in the flame. Consequently, the products of its composition have only a minor effect on the flame structure, and we concentrate the remaining discussion on CH_2F_2, and CF_3H.

Previous researchers have suggested [16, 22, 23, 27] that fluorinated compounds act to reduce the overall reaction rate through their

TABLE 2

Hydrogen, Oxygen, and Hydroxyl Radical Creation/Destruction Reactions Which Are at Least 1% of the Total Reaction Flux and Which Involve Fluorinated Species

AGENT Reaction	% of H Cons.	Reaction	% of OH Cons.	Reaction	% of O Cons.
CF_3H					
$CHF_3 + H = CF_3 + H_2$	7	$CHF_3 + OH = CF_3 + H_2O$	2	—	—
$CF_2 + H = CF + HF$	6	—	—	—	—
$CF_3 + H = CF_2 + HF$	5	$CF_3 + OH = CF_2O + HF$	2	—	—
$CFO + H = CO + HF$	3	—	—	—	—
$CF_2O + H = CFO + HF$	2	—	—	—	—
$(H_2 + F = H + HF)$	−1	$(H_2O + F = OH + HF)$	−5	—	—
		—		$CF + O_2 = CFO + O$	−12
sum:	22		−1		−12
CH_2F_2					
$CHF + H = CH + HF$	4	—	—	—	—
$CHF_2 + H = CHF + HF$	3	—	—	—	—
$CH_2F_2 + H = CHF_2 + H_2$	3	$CH_2F_2 + OH = CHF_2 + H_2O$	5	—	—
$CF_2 + H = CF + HF$	2	—	—	—	—
$CFO + H = CO + HF$	2	—	—	—	—
—	—	$(F + H_2O = OH + HF)$	−1	—	—
		—		$CF + O_2 = CFO + O$	−7
sum:	14		4		−7
CF_4					
none		none		none	

(and their decomposition products') reaction with hydrogen atoms to form less reactive radicals and ultimately HF. In order to test this hypothesis for near-stoichiometric methane-air flames with the present kinetic mechanism, we examined the peak radical concentrations, the radical concentrations in the fuel consumption zone of the flame, and the reaction fluxes for production and consumption of O, H, and OH radicals in the reaction zone. Table 2 shows the reactions involving fluorine which directly consume or create H and OH radicals in a stoichiometric flame with 4% CH_2F_2 or CF_3H. The integration of the reaction fluxes is again carried out only over the primary reaction zone of the flame. For the CF_4-inhibited flames, all of the fluorinated-species reactions affected the O, H, or OH production rates by less than 1%. However, for CF_3H and CH_2F_2, the sum of these reactions account for almost 20% of the H- and OH-atom consumption in the primary reaction zone. The direct effect of the fluorinated species reactions on OH production is negligible for CF_3H and represents only 4% of the OH consumption for CH_2F_2 (primarily through OH reaction with CH_2F_2). The production rate of O-atoms is predicted to be increased from the reaction $CF + O_2 = CFO + O$. Nonetheless, both O and OH concentrations are reduced through the additional H-atom consumption reactions and the $H_2 - O_2$ shuffle reactions. Figures 5a and 5b show the peak O, H, and OH radical concentrations for CH_2F_2- and CF_3H-inhibited flames, respectively. Also shown in the figures are the peak radical concentrations in flames at the same final temperature of the inhibited flames but in the absence of the fluorinated species (obtained through calculation with inert dilution). Clearly, the presence of CF_3H and CH_2F_2 reduces the peak radical concentrations below that due to a temperature effect alone (Figs. 5a and 5b also present the calculated final temperatures of these flames as a function of

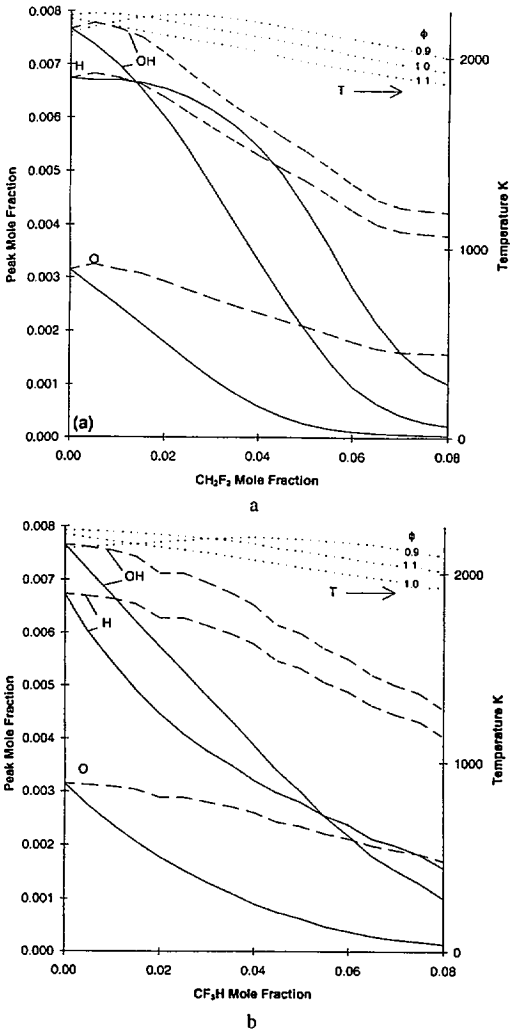

Fig. 5. Numerically calculated peak O, H, and OH mole fraction (solid lines) as a function of inhibitor mole fraction in the total reactant stream for CH_2F_2 and CF_2H added to a stoichiometric methane–air flame. Also shown (dashed lines) is the peak mole fraction of O, H, and OH in a methane–air flame at the same final temperature of the inhibited flame (obtained through addition of small quantities of an inert species). The dotted lines show the calculated final temperature.

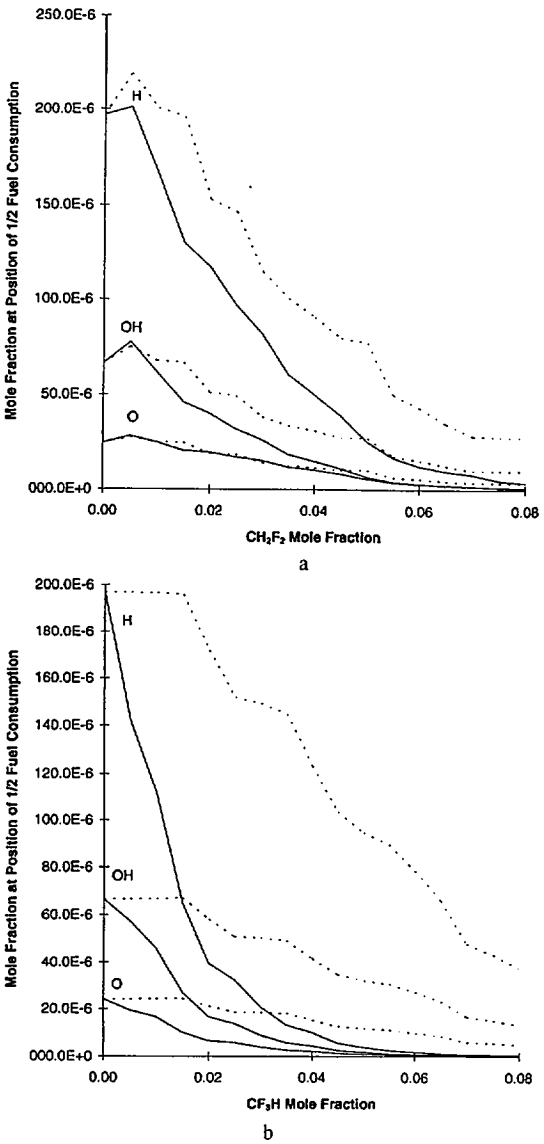

Fig. 6. Numerically calculated O, H, and OH mole fraction (solid lines) at the point one-half of the fuel consumption in a premixed stoichiometric methane–air flame to which 4% CH_2F_2 and CF_3H have been added as inhibitors, as a function of inhibitor mole fraction in the total reactant stream. The dashed lines indicate the radical mole fraction at the point of one-half fuel consumption for flames at the same final temperature as the inhibited flame (obtained through addition of small quantities of an inert species).

the inhibitor mole fraction). As discussed by Westbrook [20], the H-atom concentration in the fuel consumption region of the flame is related to the burning velocity. Figures 6a and 6b show the O, H, and OH radical concentration at the point of one-half of the fuel consumption as a function of inhibitor mole fraction in the unburned gases (two levels of interpolation between the existing numerical solutions contribute to the graininess in Figs. 6). The large reduction in the radical concentrations and the reduced rate of reduction at higher inhibitor concentrations are evident, especially for the case of CF_3H.

CONCLUSIONS

The reduction in burning velocity has been determined experimentally and numerically for the fluorinated inhibitors CF_3H, CH_2F_2, and CF_4 in near-stoichiometric premixed methane-air flames at inhibitor concentrations up to 8%. These data and analyses represent the first such measurements and calculations for these agents, fuel and conditions. The numerical results indicate that the reduced burning velocity for the flames with CF_3H and CH_2F_2 is a consequence of lower hydrogen atom concentrations occurring from reactions of H to form less reactive radicals and HF. The calculations illustrate that these inhibitors are *not* inert in the present flames and show that the burning velocity reductions and radical concentration decreases are greater than can be accounted for by temperature reduction from dilution by the inhibitors acting as inert species. Even at this early stage of development, the NIST fluorine-inhibition mechanism predicts the burning velocity reduction quite well for these flames. Further research is necessary to validate the mechanism with other flames and with more stringent comparisons than burning velocity (such as detailed flame structure measurements). As the mechanism is further developed and refined, better agreement for CF_3H-inhibition of methane–air flames should be possible, and the mechanism can be extended to larger fuels and inhibitors.

This research was supported by the US Naval Air Systems Command; US Army Aviation and Troop Command; Federal Aviation Administration Technical Center; and the US Air Force. The authors especially appreciate the support and technical direction of Mr. J. Michael Bennett at the Wright Patterson AFB Flight Dynamics Laboratory, Survivability Enhancement Branch. The authors are grateful to Drs. D. Burgess, W. Tsang, P. Westmoreland, and M. Zachariah for helpful conversations and for making their mechanism and publications available prior to publication; to Drs. J. Vandooren and P. Van Tiggelen for helpful suggestions concerning the experimental techniques; and to Dr. J. Hodges for help with the image processing. The assistance of Mr. Arnold Liu and Miss Cynthia Yu in writing the data acquisition and image processing software, performing the numerical calculations, and reducing the data is gratefully acknowledge.

REFERENCES

1. Gann, R. G. (Ed.), *Halogenated Fire Suppressants*. ACS Symposium Series No. 16, The American Chemical Society, Washington, D.C., 1975.
2. Hastie, J. W., *High Temperature Vapors: Science and Technology*, Academic Press, New York, 1975, p. 332.
3. Burgoyne, J. H., and Williams-Lier, G., *Proc. R. Soc. A* 193:525–539 (1948).
4. Coleman, E. H., *Fuel* 30:114–115 (1951).
5. Belles, F. E., and O'Neal, C. Jr., *Sixth Symposium (International) on Combustion*, The Combustion Institute, Pittsburgh, 1956, p. 806.
6. Simmons, R. F., and Wolfhard, H. G., *Trans. Farad. Soc.* 52:53–59 (1956).
7. Garner, F. H., Long, R., Graham, A. J., and Badakhshan, A., *Sixth Symposium (International) on Combustion*. The Combustion Institute, Pittsburgh, 1957, p. 802.
8. Rosser, W. A., Wise, H., and Miller, J., *Seventh Symposium (International) on Combustion*., Butterworths, London, 1959, p. 175.
9. Lask, G., and Wagner, H. G., *Eighth Symposium (International) on Combustion*, Williams & Wilkins, Baltimore, 1962, p. 432.
10. Niioka, T., Mitani, T., and Takahashi, M., *Combust. Flame* 50:89–97 (1983).
11. Mitani, T., *Combust Flame* 50:177–188 (1983).
12. Levy, A., Droege, J. W., Tighe, J. J., and Foster, J. F., *Eighth Symposium (International) on Combustion*, Williams & Wilkins, Baltimore, 1962, p. 524.
13. Wilson, W. E., Jr., *Tenth Symp. (International) on Combustion*, The Combustion Institute, Pittsburgh, 1965, p. 47.
14. Wilson, W. E., O'Donovan, J. T., and Fristrom, R. M., *Twelfth Symposium (International) on Combustion*, The Combustion Institute, Pittsburgh, 1969, p. 929.
15. Biordi, J. C., Lazzara, C. P., and Papp, J. F., *Fourteenth Symposium (International) on Combustion*, The Combustion Institute, Pittsburgh, 1973, p. 367.
16. Biordi, J. C., Lazzara, C. P., and Papp, J. F., *Fifteenth Symposium (International) on Combustion*, The Combustion Institute, Pittsburgh, 1975, p. 917.
17. Safieh, H. Y., Vandooren, and Van Tiggelen, P. J., *Nineteenth Symposium (International) on Combustion*, The Combustion Institute, Pittsburgh, 1982, p. 117.
18. Day, M. J., and Stamp, D. V., Thompson, K., and Dixon-Lewis, G., *Thirteenth Symposium (International) on Combustion*, The Combustion Institute, Pittsburgh, 1971, p. 705.
19. Dixon-Lewis, G., and Simpson, R. J., *Sixteenth Symposium (International) on Combustion*, The Combustion Institute, Pittsburgh, 1977, p. 1111.
20. Westbrook, C. K., *Combust. Sci. Technol.* 23:191–202 (1980).
21. Westbrook, C. K., *Nineteenth Symp. (International) on*

Combustion, The Combustion Institute, Pittsburgh, 1982, p. 127.
22. Westbrook, C. K., *Combust. Sci. Technol.* 34:201–225 (1983).
23. Vandooren, J., da Cruz, F. N., and Van Tiggelen, P. J., *Twenty-second Symposium (International) on Combustion*, The Combustion Institute, Pittsburgh, 1988, p. 1587.
24. da Cruz, F. N., Vandooren, J., and Van Tiggelen, P., *Bull. Soc. Chim. Belg.* 97:11–12, 1001–1030 (1988).
25. Sheinson, R. S., and Baldwin, S. P., Halon Alternatives Technical Working Conference, Albuquerque, NM, May 11–13, 1993, p. 493.
26. Sheinson, R. S., Penner-Hahn, J. E., Indritz, D., *Fire Safety J.* 15:437–450, 1989.
27. Richter, H., Vandooren, J., and Van Tiggelen, P., *Bull. Soc. Chim. Belg.* 99:7, 491–501 (1990).
28. Linnett, J. W., *Fourth Symposium (International) on Combustion*. Williams & Wilkins, Baltimore, 1953, p. 20.
29. Andrews, G. E., and Bradley, D., *Combust. Flame* 18:133–153 (1972).
30. Mache, H., and Hebra, A., *Sitzungsber. Osterreich. Akad. Wiss., Abt.* IIa, 150, 157 (1941).
31. Van Wonterghem, J., and Van Tiggelen, A., *Bull. Soc. Chim. Belg.* 63, 235–260 (1954).
32. Kee, R. J., Miller, J. A., and Jefferson, T. H., Sandia National Laboratories Report, 1980, SAND80-8003.
33. Kee, R. J., Warnatz, J., and Miller, J. A., Sandia National Laboratories Report, 1983, SAND83-8209.
34. Kee, R. J., Grcar, J. F., Smooke, M. D., and Miller, J. A. A Fortran Computer Program for Modeling Steady Laminar One-dimensional Premixed Flames, *Sandia National Laboratories Report*, SAND85-8240, 1991.
35. Burgess, D. R. F., Jr., Zachariah, M. R., Tsang, W., and Westmoreland, P. R., *Natl. Inst. of Std. Technol.*, submitted.
36. Burgess, D. R. F., Jr., Zachariah, M. R., Tsang, W., and Westmoreland, P. R., Thermochemical and Chemical Kinetic Data for Fluorinated Hydrocarbons, special issue of *Prog. Ener. Combust. Sci.* (in press).
37. Burgess, D., Jr., Tsang, W., Westmoreland, P. R., Zachariah, M. R., Third International Conference on Chemical Kinetics, July 12–16, 1992, Gaithersburg, MD, 1993, p. 119.
38. Westmoreland, P. R., Burgess, D. F. R., Jr., Tsang, W., and Zachariah, M. R., *Twenty-Fifth Symposium (International) on Combustion*, The Combustion Institute, Pittsburgh, 1994.
39. Nyden, M. R., Linteris, G. T., Burgess, D. R. F., Jr., Westmoreland, P. R., Tsang, W., and Zachariah, M. R., in *Evaluation of Alternative In-Flight and Dry Bays* (W. L. Grosshandler, R. G. Gann, and W. M. Pitts, Eds.), National Institute of Standards and Technology, Gaithersburg, MD, 1994, NIST SP 861, p. 467.
40. Frenklach, M., Wang, H., Bowman, C. T., Hanson, R. K., Smith, G. P., Golden, D., Gardiner, W., Lissianski, V., presented at the Twenty-fifth Symposium (International) on Combustion, Poster 3-26.
41. Linteris, G. T., and Truett, L. F., Presented at the Halon Options Technical Working Conference, Albuquerque, NM, May 3–5, 1994, p. 227.
42. Linteris, G. T., and Truett, L. F., Eastern States Section Meeting, Clearwater Beach, FL, Dec. 5–7, 1994, The Combustion Institute, Pittsburgh, 1994, p. 385.
43. Vagelopoulos, C. M., Egolfopoulos, F. N., and Law, C. K., *Twenty-fifth Symposium (International) on Combustion*, The Combustion Institute, Pittsburgh, 1994, p. 1341.

Received 30 December 1994; revised 20 June 1995